How to cite: *Angew. Chem. Int. Ed.* **2024**, *63*, e202318254
doi.org/10.1002/anie.202318254

Polycyclic Aromatic Hydrocarbons

π-Radical Cascade to a Chiral Saddle-Shaped Peropyrene

Annika Bernhardt, Daniel Čavlović, Maximilian Mayländer, Olivier Blacque, Carlos M. Cruz, Sabine Richert,* and Michal Juríček**

Dedicated to Marcel Mayor

Abstract: Reactions of open-shell molecular graphene fragments are typically thought of as undesired decomposition processes because they lead to the loss of desired features like π-magnetism. Oxidative dimerization of phenalenyl to peropyrene shows, however, that these transformations hold promise as a synthetic tool for making complex structures via formation of multiple bonds and rings in a single step. Here, we explore the feasibility of using this "undesired" reaction of phenalenyl to build up strain and provide access to non-planar polycyclic aromatic hydrocarbons. To this end, we designed and synthesized a biradical system with two phenalenyl units linked via a biphenylene backbone. The design facilitates an intramolecular cascade reaction to a helically twisted saddle-shaped product, where the key transformations—ring-closure and ring-fusion—occur within one reaction. The negative curvature of the final peropyrene product, induced by the formed eight-membered ring, was confirmed by single-crystal X-ray diffraction analysis and the helical twist was validated via resolution of the product's enantiomers that display circularly polarized luminescence and high configurational stability.

Phenalenyl[1] (**PLY**)—the smallest molecular fragment of graphene that hosts an unpaired electron—decomposes in air or in the presence of an oxidant to a fused dimeric product, peropyrene (**PP**; Figure 1). This five-step π-radical cascade is a rare case of a well-understood decomposition pathway[2,3] of triangular graphene fragments,[4] compounds that are primarily explored for their π-magnetism[5–9] and as building blocks[10,11] of quantum materials. But is this transformation, in which two σ-bonds, one π-bond, and a new ring are formed in a single reaction, destined to carry the label[2] "decomposition" or is it time to change this paradigm and embrace this kind of reactions as synthetically useful?

Let us rethink the π-radical cascade of phenalenyl and look at this typically undesired process through the lens of methodology. The unpaired π-electron in **PLY** is uniformly delocalized over the six α-positions,[12] and even though this provides partial thermodynamic stabilization, **PLY** undergoes facile oxidative dimerization. The first step of this

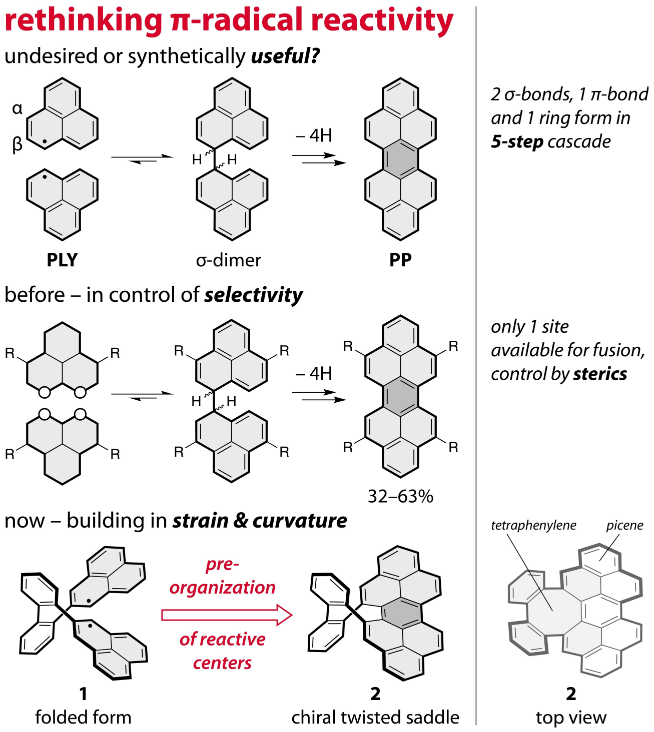

Figure 1. Oxidative dimerization of phenalenyl (**PLY**) gives peropyrene (**PP**) in five steps[2,3] (top). The selectivity of this π-radical cascade can be controlled by sterics[19,20] (middle), but here we show that we can also employ it to build up strain and access saddle-shaped geometries (bottom).

---

[*] Dr. A. Bernhardt, Dr. D. Čavlović, Dr. O. Blacque, Dr. C. M. Cruz, Prof. M. Juríček
Department of Chemistry, University of Zurich
Winterthurerstrasse 190, 8057 Zurich (Switzerland)
E-mail: michal.juricek@chem.uzh.ch

M. Mayländer, Dr. S. Richert
Institute of Physical Chemistry, University of Freiburg
Albertstraße 21, 79104 Freiburg (Germany)
E-mail: sabine.richert@physchem.uni-freiburg.de

Dr. C. M. Cruz
Department of Organic Chemistry, University of Granada
Avenida de la Fuente Nueva S/N, 18071 Granada (Spain)
E-mail: cmorenoc@ugr.es

process is the reversible formation of a σ-dimer[13] (Figure 1, top), which can occur at each α-position with equal probability. To suppress the reactivity of **PLY**, we must either increase its thermodynamic stability, as in 1,9-dithio-**PLY**,[14] or provide sufficient kinetic stabilization, which can be achieved[15,16] by installation of bulky substituents that block all reactive positions. For example, three *tert*-butyl groups placed at the β-positions of **PLY** shield all α-positions sterically and fully suppress[17] the first step of the cascade. Alternatively, molecular isolation enables[5–9] studies of pristine systems on surfaces under ultra-high vacuum. If, on the other hand, we want to unleash the reactivity and use π-radical cascades as a synthetic tool, the **PLY**'s π-delocalized electronic structure offers a unique opportunity to make some positions more reactive than others and thereby enable selectivity control. This principle was demonstrated intermolecularly using steric effects[18–20] (Figure 1, middle) and π-extension,[21] as well as intramolecularly in oligomeric **PLY**-based systems.[22,23]

To demonstrate that this and related reactions hold a transformative potential for synthesis, we set out to explore if it is possible to utilize the oxidative dimerization of **PLY** to access curved polycyclic aromatic hydrocarbons. Even though the synthesis of distorted structures requires the build-up of strain,[24] we reasoned that such a transformation should be feasible because of the gain of aromatic stabilization energy (Figure 1, dark-gray ring) in the final step of the **PLY** cascade. Following this idea, we designed biradical **1** (Figure 1, bottom) in which two **PLY** units (gray fill) are linked via their β-positions using a 2,2′-biphenylene spacer (white fill) to give an eight-membered ring upon their intramolecular ring-fusion (dark-gray fill). Calculations (DFT/M05-2X/6-31G(d,p), Figure S58) revealed that the expected product, picenotetraphenylene (**2**), possesses a chiral saddle-geometry with a strain energy of ~12 kcal mol^{-1} (Table S10) and features a twisted peropyrene unit. Here, we demonstrate that this concept works and report[25] insights into this π-radical cascade process, as well as the characterization of the final product **2**.

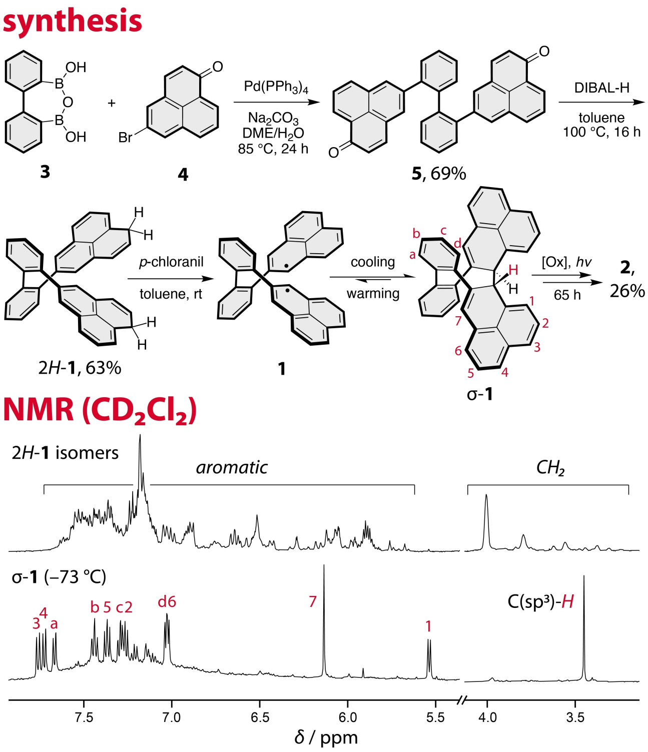

Figure 2. Synthesis and ^{1}H NMR spectrum of precursor 2*H*-**1**, and its oxidation with one equivalent of *p*-chloranil to biradical **1** that is in thermal equilibrium with its σ-dimer (σ-**1**) observed by ^{1}H NMR spectroscopy at −73 °C.

The dihydro-precursor of biradical **1**, compound 2*H*-**1**, was prepared via a convergent synthesis with nine steps in the longest linear sequence (Figure 2). 2,2′-Biphenylene was selected as the linking unit as it provides enough rigidity to achieve the desired selectivity of the σ-dimerization step but leaves enough flexibility for the remaining steps of the cascade to proceed. The 2,2′-biphenylene building block **3**[26] was synthesized by treating 1,2-dibromobenzene with *n*-butyllithium followed by trimethyl borate (see the SI). The second building block, phenalenone **4**, was prepared from naphthalene in six steps, as described[27] previously. A twofold Suzuki coupling of **3** with two equivalents of **4** was employed to afford diketone **5** whose structure was validated by X-ray crystallography[28] (Figure S25). Subsequently, **5** was reduced with DIBAL–H to give the air-sensitive dihydro-precursor 2*H*-**1** in a 43 % yield over the two steps. Similar to other related systems, 2*H*-**1** was obtained as a mixture of regioisomers, which differ from each other in the location of the methylene groups in the phenalene unit, as observed by NMR spectroscopy (Figure 2) and HRMS (see the commentary in the SI, X-Ray Crystallography section[28]). The target biradical **1** was generated by oxidation of 2*H*-**1** with *p*-chloranil and directly used for the subsequent experiments without further purification. All experiments involving 2*H*-**1** and biradical **1** were performed under inert conditions.

The transformation of 2*H*-**1** to **2** was monitored by several spectroscopic techniques, including NMR, EPR, and UV/Vis, which allowed the observation of three out of four intermediates of this oxidative cascade. Upon the addition of one equivalent of *p*-chloranil (the theoretical amount needed for the removal of two hydrogen atoms), the ^{1}H NMR signals that belong to 2*H*-**1** disappear (Figure S12), indicating the formation of biradical species **1**. Upon cooling of this mixture, new signals start to appear and at −73 °C, a well-resolved spectrum is obtained (Figure 2). This process is reversible and upon warming, the original spectrum is restored. This behavior supports the expected equilibrium between **1** and its intramolecular σ-dimer (σ-**1**). Indeed, the assignment of proton and carbon resonances using 2D NMR spectroscopy at −73 °C in CD$_2$Cl$_2$ (see the SI) confirms the structure of σ-**1** that is present in the form of a single diastereomer (*RR*/*SS*).

The presence of the biradical species **1** was probed by continuous-wave EPR spectroscopy in toluene ($c \approx 10^{-4}$ M), revealing a signal with a pronounced hyperfine structure (a triplet of a septet) and an isotropic g value of 2.0025 (Figure 3, top). Interestingly, the experimental proton

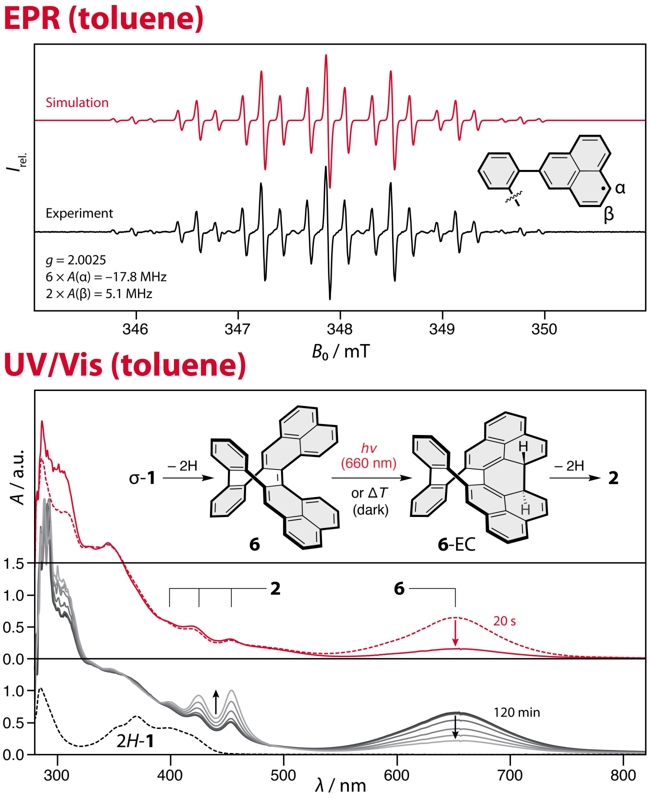

Figure 3. (top) EPR spectrum of a toluene solution of 2*H*-**1** and one equivalent of *p*-chloranil. (bottom) Observation of intermediate **6** ($\lambda_{\max}$ = 654 nm) by UV/Vis spectroscopy and its thermal (black trace) and photochemical (red trace) decay at room temperature in toluene.

hyperfine coupling constants ($A = -17.8$ and 5.1 MHz) do not match the values calculated for the triplet **1** (Figure S45), but those calculated for the partially oxidized monoradical species *H*-**1** ($A = -16.6$ and 6.8 MHz, DFT/U-M05-2X/EPR-III on M05-2X/6-31G(d,p) geometries, Figure S44). Moreover, the signal is near-identical to that obtained for the reference molecule β-phenyl-**PLY**, which represents one half of **1** (Figure S28a). The only difference is that the intrinsic linewidth seems to be smaller in the case of the reference molecule, so that the additional smaller proton hyperfine couplings become visible.

These results point toward the presence of either (i) monoradical species *H*-**1** or (ii) biradical species **1** with a negligible spin–spin coupling between the two **PLY** units. The following experimental observations support the second case: varying the amount of oxidant down to substoichiometric amounts results in (1) an identical EPR signal (Figure S28b) and (2) the appearance of NMR signals that correspond to σ-**1** at −73 °C, (3) the EPR signal disappears at temperatures below 230 K and appears again when the temperature is raised (Figure S28c), (4) the NMR signals of σ-**1** appear at lower temperatures and broaden at room temperature (Figure S12); (3) and (4) endorse the equilibrium between **1** and σ-**1**. The DFT calculations further support this scenario and observations. The energy difference between broken-symmetry (BS)-singlet **1** and triplet **1** is <0.01 and 0.12 kcal mol^{-1} (in favor of the singlet state, U-M05-2X/6-31G(d,p); Tables S4 and S5) for the unfolded and folded conformations, respectively. This indicates a diminished spin–spin interaction, on account of the disrupted conjugation due to orthogonality of the biphenylene linker. The energy of σ-**1** is lower by 3.81 kcal mol^{-1} with respect to the folded BS-singlet **1** (Figure S50).

The next intermediate of the cascade, namely, compound **6**, was observed by UV/Vis spectroscopy after the addition of an equivalent amount of *p*-chloranil to 2*H*-**1** (Figure 3, bottom). A new broad absorption band ($\lambda_{\max} = 654$ nm) appeared instantly and its intensity increased in time until it reached a maximum after 20 min, then it slowly decreased again (black trace). Upon irradiation at 660 nm for 20 s, the band at 654 nm disappears instantly (red trace). These results are consistent with a biphenalenylidene-type intermediate **6**, which undergoes both thermal and photochemical electrocyclization to **6**-EC (see the SI, page S45) on account of its small HOMO–LUMO gap and diradicaloid character, similar to biphenalenylidene[2] and cethrene.[29] The TD-DFT calculations for **6** are in agreement with the absorption profile (Tables S6 and S7, Figures S54 and S55) and the energetically favored electrocyclic process (**6**-EC is lower in energy compared to **6**, see Figures S56 and S57). Even though **6**-EC could not be observed directly, its intermediacy is supported by the observation that the absorption bands of the final product **2** do not appear instantly after irradiation (Figure 3, bottom, red trace). In contrast, the appearance of these bands is simultaneous with the decrease of the band at 654 nm (**6**) during the thermal process (black trace). The overall cascade can be performed under both thermal and photochemical reaction conditions, with the latter process being faster. Even though no major side-products were observed, the isolated yield of the final product **2** was 28 % over five consecutive steps (~78 % per step).

The structure of **2** was elucidated by means of 2D NMR spectroscopy (Figures S13–S17) and X-ray diffraction analysis[28] (Figure 4, top left), revealing a twisted saddle-shape geometry. The structure of **2** is strained (12.2 kcal mol^{-1}), as estimated using a homodesmotic reaction (Figure S62). The UV/Vis absorption and emission spectra of **2** resemble the features of the spectra obtained previously[19] for a flat **PP** derivative and reveal a Stokes shift of 589 cm^{-1} ($\lambda_{\mathrm{abs}} = 463$ nm, $\lambda_{\mathrm{em}} = 476$ nm; Figure 4, top right). The fluorescence quantum yield (Φ_{F}) of **2** is 68 %. With the help of TD-DFT, the lowest-energy absorption band was assigned to the main HOMO→LUMO transition ($\lambda = 461.04$ nm, $f = 0.9553$; CAM-B3LYP/6-31G(d,p)/PCM on M05-2X/6-31G(d,p) geometry, correction –0.25 eV), with the frontier molecular orbitals resembling those of pristine **PP** (Figure S59). As a result of its rigid twisted geometry, **2** is chiral and its enantiomers could be resolved using chiral-stationary-phase high-performance liquid chromatography (HPLC; Figure 4, bottom left). The enantiomers displayed mirror-image Cotton effects in their circular dichroism (CD) spectra (Figure 4, bottom right) and their configuration was assigned using TD-DFT calculated transitions (Figure S61). Enantioenriched samples of **2** exhibited circularly polarized luminescence (CPL) in the range of 450–600 nm with a

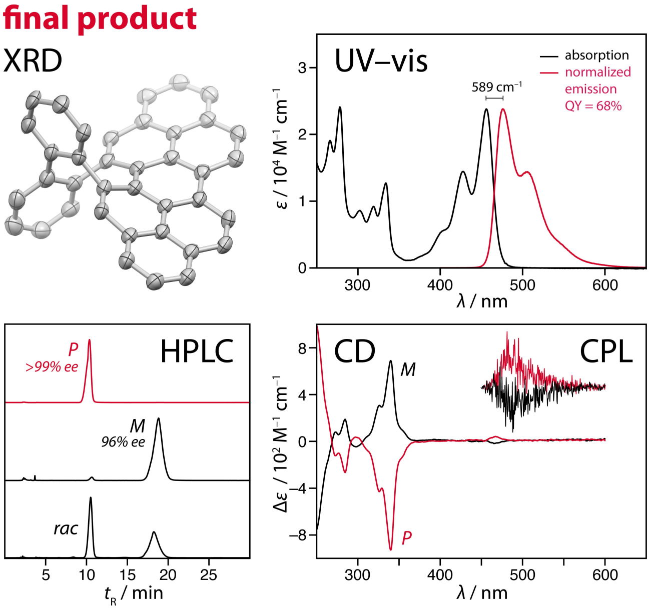

Figure 4. (top left) Solid-state structure of **2** with the thermal ellipsoids shown at 50% probability level and the hydrogen atoms omitted for clarity. (top right) Absorption and normalized emission spectra of **2** (10^{-5} M in CH_2Cl_2) at 298 K. (bottom left) Chiral-stationary-phase HPLC traces of (*P*)-**2**, (*M*)-**2**, and (±)-**2** (Reprosil Chiral-MIA, hexanes/*i*-PrOH (99:1), 1.5 mL/min). (bottom right) CD and CPL spectra of (*P*)- and (*M*)-**2** (10^{-5} M in CH_2Cl_2, $\lambda_{exc}=370$ nm).

luminescence dissymmetry factor (g_{lum}) of 2×10^{-4}, which is comparable to other[30] chiral peropyrenes. A high enantiomerization barrier is predicted by DFT (~63 kcal mol^{-1}, M05-2X/6-31G(d,p)), consistent with observation that no racemization occurs at 80 °C (Figure S35). The calculated barrier is in the range of barriers for related benzannulated cyclooctatetraenes suffering from multiple bay-region clashes[31] and is on the high end among chiral polycyclic aromatic systems.[30,32]

Our study illustrates that we can leverage the typically undesired π-radical reactivity as a method for making novel functional materials—not only by building extended aromatic cores but also via inducing strain to access curved systems. The **PLY** cascade complements the rather limited pool of methods toward chiral peropyrenes,[30,32–34] while the contortion of the **PP** unit makes compound **2** a promising singlet-fission material, as highlighted recently for bent pyrenacene[35] and rylene diimide[36] families. Moreover, by controlling the amount of oxidant, we could showcase a reversible two-state thermal magnetic switch, which is relevant in the context of responsive materials[37] for spintronics.

Acknowledgements

This project received funding from the European Research Council (ERC) under the European Union's Horizon 2020 research and innovation programme (M.J./716139, INSPIRAL), the Swiss National Science Foundation (SNSF; C.M.C./CRSK-2_190365, M.J./PP00P2_170534, PP00P2_198900 and TMCG-2_213829, CASCADER) and the University of Zurich (UZH; C.M.C./FK-21-131). S.R. acknowledges support by the Deutsche Forschungsgemeinschaft (DFG, German Research Foundation)—Project number 417643975. We would like to thank the S^{3}IT team (www.s3it.uzh.ch, the Service and Support for Science IT team at UZH) for their support and use of the infrastructure, and Prof. Marcel Mayor (University of Basel), to whom this manuscript is dedicated, for his continuous support and fruitful discussions during the PhD committee meetings of A.B. Open Access funding provided by Universität Zürich.

Conflict of Interest

The authors declare no conflict of interest.

Data Availability Statement

The data that support the findings of this study are openly available in https://zenodo.org at 10.5281/zenodo.10212222, reference number 10212222.

Keywords: phenalenyl · biradicals · peropyrene · negative curvature · circularly polarized luminescence

---

[1] D. H. Reid, *Q. Rev. Chem. Soc.* **1965**, *19*, 274–302.
[2] K. Uchida, S. Ito, M. Nakano, M. Abe, T. Kubo, *J. Am. Chem. Soc.* **2016**, *138*, 2399–2410.
[3] S. Pogodin, I. Agranat, *J. Am. Chem. Soc.* **2003**, *125*, 12829–12835.
[4] Y. Morita, S. Suzuki, K. Sato, T. Takui, *Nat. Chem.* **2011**, *3*, 197–204.
[5] E. Turco, A. Bernhardt, N. Krane, L. Valenta, R. Fasel, M. Juríček, P. Ruffieux, *JACS Au* **2023**, *3*, 1358–1364.
[6] N. Pavliček, A. Mistry, Z. Majzik, N. Moll, G. Meyer, D. Fox, L. Gross, *Nat. Nanotechnol.* **2017**, *12*, 308–311.
[7] S. Mishra, D. Beyer, K. Eimre, J. Liu, R. Berger, O. Gröning, C. A. Pignedoli, K. Müllen, R. Fasel, X. Feng, P. Ruffieux, *J. Am. Chem. Soc.* **2019**, *141*, 10621–10625.
[8] J. Su, M. Telychko, P. Hu, G. Macam, P. Mutombo, H. Zhang, Y. Bao, F. Cheng, Z.-Q. Huang, Z. Qiu, S. J. R. Tan, H. Lin, P. Jelínek, F.-C. Chuang, J. Wu, J. Lu, *Sci. Adv.* **2019**, *5*, eaav7717.
[9] S. Mishra, K. Xu, K. Eimre, H. Komber, J. Ma, C. A. Pignedoli, R. Fasel, X. Feng, P. Ruffieux, *Nanoscale* **2021**, *13*, 1624–1628.
[10] S. Mishra, G. Catarina, F. Wu, R. Ortiz, D. Jacob, K. Eimre, J. Ma, C. A. Pignedoli, X. Feng, P. Ruffieux, J. Fernández-Rossier, R. Fasel, *Nature* **2021**, *598*, 287–292.
[11] J. Hieulle, S. Castro, N. Friedrich, A. Vegliante, F. R. Lara, S. Sanz, D. Rey, M. Corso, T. Frederiksen, J. I. Pascual, D. Peña, *Angew. Chem. Int. Ed.* **2021**, *60*, 25224–25229.
[12] P. B. Sogo, M. Nakazaki, M. Calvin, *J. Chem. Phys.* **1957**, *26*, 1343–1345.
[13] F. Gerson, *Helv. Chim. Acta* **1966**, *49*, 1463–1467.
[14] R. C. Haddon, F. Wudl, M. L. Kaplan, J. H. Marshall, R. E. Cais, F. B. Bramwell, *J. Am. Chem. Soc.* **1978**, *100*, 7629–7633.
[15] S. Arikawa, A. Shimizu, D. Shiomi, K. Sato, R. Shintani, *J. Am. Chem. Soc.* **2021**, *143*, 19599–19605.

[16] L. Valenta, M. Mayländer, P. Kappeler, O. Blacque, T. Šolomek, S. Richert, M. Juríček, *Chem. Commun.* **2022**, *58*, 3019–3022.
[17] K. Goto, T. Kubo, K. Yamamoto, K. Nakasuji, K. Sato, D. Shiomi, T. Takui, M. Kubota, T. Kobayashi, K. Yakusi, J. Ouyang, *J. Am. Chem. Soc.* **1999**, *121*, 1619–1620.
[18] L. Beer, S. K. Mandal, R. W. Reed, R. T. Oakley, F. S. Tham, B. Donnadieu, R. C. Haddon, *Cryst. Growth Des.* **2007**, *7*, 802–809.
[19] Y. Yang, O. Blacque, S. Sato, M. Juríček, *Angew. Chem. Int. Ed.* **2021**, *60*, 13529–13535.
[20] Y. Yang, S. Huangfu, S. Sato, M. Juríček, *Org. Lett.* **2021**, *23*, 7943–7948.
[21] D. Čavlović, D. Häussinger, O. Blacque, P. Ravat, M. Juríček, *JACS Au* **2022**, *2*, 1616–1626.
[22] T. Shen, Y. Zou, X. Hou, H. Wei, L. Ren, L. Jiao, J. Wu, *Angew. Chem. Int. Ed.* **2023**, *62*, e20231192.
[23] T. Jiao, Y. Ni, T. Xu, X. Hou, S. Wu, L. Ren, Y. Gu, X. Miao, Z. Sun, J. Wu, *Nat. Synth.* **2023**, *2*, 1104–1115.
[24] M. A. Majewski, M. Stępień, *Angew. Chem. Int. Ed.* **2019**, *58*, 86–116.
[25] Raw data are available at Zenodo: https://zenodo.org/record/10212222.
[26] A. Das, A. Hübner, M. Weber, M. Bolte, H.-W. Lerner, M. Wagner, *Chem. Commun.* **2011**, *47*, 11339–11341.
[27] N. Krane, E. Turco, A. Bernhardt, D. Jacob, G. Gandus, D. Passerone, M. Luisier, M. Juríček, R. Fasel, J. Fernández-Rossier, P. Ruffieux, *Nano Lett.* **2023**, *23*, 9353–9359.
[28] Deposition numbers 2309903 (**5**), 2309905 (2*H*-**1**), and 2309910 (**2**) contains the supplementary crystallographic data for this paper. These data are provided free of charge by the joint Cambridge Crystallographic Data Centre and Fachinformationszentrum Karlsruhe Access Structures service.
[29] P. Ravat, T. Šolomek, M. Rickhaus, D. Häussinger, M. Neuburger, M. Baumgarten, M. Juríček, *Angew. Chem. Int. Ed.* **2016**, *55*, 1183–1186.
[30] W. Yang, G. Longhi, S. Abbate, A. Lucotti, M. Tommasini, C. Villani, V. J. Catalano, A. O. Lykhin, S. A. Varganov, W. A. Chalifoux, *J. Am. Chem. Soc.* **2017**, *139*, 13102–13109.
[31] For example: P. Rashidi-Ranjbar, Y. M. Man, J. Sandstroem, H. N. C. Wong, *J. Org. Chem.* **1989**, *54*, 4888–4892.
[32] H. V. Anderson, N. D. Gois, W. A. Chalifoux, *Org. Chem. Front.* **2023**, *10*, 4167–4197.
[33] W. Yang, J. H. S. K. Monteiro, A. de Bettencourt-Dias, V. J. Catalano, W. A. Chalifoux, *Angew. Chem. Int. Ed.* **2016**, *55*, 10427–10430.
[34] K. M. Magiera, V. Aryala, W. A. Chalifoux, *Org. Biomol. Chem.* **2020**, *18*, 2372–2386.
[35] C. M. Cruz, J. C. Walsh, M. Juríček, *Org. Mater.* **2022**, *4*, 163–169.
[36] C. Schaack, A. M. Evans, F. Ng, M. L. Steigerwald, C. Nuckolls, *J. Am. Chem. Soc.* **2022**, *144*, 42–51.
[37] M. E. Itkis, X. Chi, A. W. Cordes, R. C. Haddon, *Science* **2002**, *296*, 1443–1445.

Manuscript received: November 29, 2023
Accepted manuscript online: January 26, 2024
Version of record online: February 29, 2024